New Journal of Physics
The open-access journal for physics

Competing exciton localization effects due to disorder and shallow defects in semiconductor alloys

C P Dietrich[1], M Lange, G Benndorf, J Lenzner, M Lorenz and M Grundmann

Institut für Experimentelle Physik II, Universität Leipzig, D-04103 Leipzig, Germany
E-mail: c.dietrich@physik.uni-leipzig.de

New Journal of Physics **12** (2010) 033030 (10pp)
Received 8 November 2009
Published 16 March 2010
Online at http://www.njp.org/
doi:10.1088/1367-2630/12/3/033030

Abstract. We demonstrate that excitons in semiconductor alloys are subject to competing localization effects due to disorder (random potential fluctuations) and shallow point defects (impurities). The relative importance of these effects varies with alloy chemical composition, impurity activation energy as well as temperature. We evaluate this effect quantitatively for $Mg_xZn_{1-x}O:Al$ ($0 \leqslant x \leqslant 0.058$) and find that exciton localization at low (2 K) and high (300 K) temperatures is dominated by shallow donor impurities and alloy disorder, respectively.

Contents

[1] Author to whom any correspondence should be addressed.

1. Introduction

Semiconductor alloys are at the core of current semiconductor technology for electronic and photonic applications. Over 50 different alloys have been investigated [1]. They offer tunable structural, optical and electronic properties through mixing constituents in a defined ratio. Besides, as bulk material they are mostly used as active and/or barrier materials in heterostructures.

The random placing of metal atoms on the cation sublattice leads to potential fluctuations and, subsequently, to the disorder-induced broadening of spectral lines (alloy broadening) as discussed in [2, 3]. We note that ordered alloys have also been reported [4]. The spectral broadening σ (half-width $w = 2.36\,\sigma$) of an alloy of the type $A_xB_{1-x}C$ with disorder on the cation lattice is given by $\sigma = (\partial E_g/\partial x)\,\sigma_x$, with x being the mole fraction, E_g being the band gap and $\sigma_x = x\,(1-x)/(cV_{exc})$, c being the cation concentration and $V_{exc} = 10\pi a_B$ being the exciton volume [3]. Broadening in $Al_xGa_{1-x}As$, a semiconductor alloy of large importance in combination with GaAs due to small lattice mismatch, has been investigated [5] and critically discussed [6]. Work on several group-II sulfide, telluride and selenide alloys has been reviewed in [7], highlighting that larger broadening is due to anion disorder rather than cation disorder. Here, we focus on cation disorder. For S-, Se- and Te-compounds, the inhomogeneous broadening σ is fairly small, e.g. for $Zn_{0.1}Cd_{0.9}S$, $Zn_{0.1}Cd_{0.9}Se$ and $Zn_{0.1}Cd_{0.9}Te$, less than 1 meV [7]. In recent years, investigations of wide-gap semiconductor alloys were reported, e.g. on $Al_xGa_{1-x}N$ [8, 9], $Al_xIn_{1-x}N$ [10, 11] and $Mg_xZn_{1-x}O$ [12, 13]. Here, inhomogeneous broadening due to cation disorder is much larger, e.g. about 30 meV for $Al_{0.2}Ga_{0.8}N$ [14], 130 meV for $In_{0.2}Al_{0.8}N$ [15] and 17 meV for $Mg_{0.2}Zn_{0.8}O$ [13].

Recombination of free excitons (FX) localized in the alloy (cation) disorder potential has been claimed, e.g. for $Zn_xCd_{1-x}S$ [16]. The exciton relaxation kinetics in the presence of potential fluctuations has been investigated for quantum wells (laterally varying confinement effect) [17] and quantum dot ensembles (varying quantum dot size) [18]. In general, a red-shift $S = \gamma(T)\,k_BT$ of luminescence compared to absorption in such an inhomogeneously broadened system is found [19]. The simplest model for the so-called Stokes shift S is based on the Boltzmann population (temperature T) of a density of states with Gaussian broadening (standard deviation σ), resulting in $S_0 = \sigma^2/k_BT$ and thus $\gamma_0 = (\sigma/k\,T)^2$. The establishment of a thermal exciton distribution is frustrated at low temperatures by trapping of excitons in potential minima and recombination, both being temperature dependent as pointed out for quantum wells [17] and dots [20]. Therefore, generally $S \leqslant S_0$. Within an analytical model [21], γ $(0 \leqslant \gamma \leqslant \gamma_0)$ can be determined from $\gamma \exp\gamma = \beta(\gamma_0 - \gamma)\exp(-\epsilon/k_BT)$, ϵ being the mean barrier for exciton transport and β being the ratio of carrier recombination and carrier transport time.

The photoluminescence (PL) peak energy due to FX is given as

$$E_X(T) = E_g(T) - E_X^b - S(T). \tag{1}$$

With decreasing temperature, first E_X exhibits a blue-shift due to the increase of band gap E_g. Then thermalization in the disordered system leads to the red-shift S. Finally, due to frustration of thermalization at low temperatures another blue-shift occurs, sometimes termed the 'anomalous' Stokes shift. This S-shape dependence of PL peak energy versus temperature is used as a fingerprint of frustrated exciton localization in quantum wells. Such S-shape of $E_{PL}(T)$ is also observed in semiconductor alloys and used to evaluate exciton localization

Table 1. Exciton binding energy, impurity localization energy and full-width at half-maximum ($w = 2.36\,\sigma$, best known values) of low-temperature recombination for various binary compound semiconductors and ternary alloys.

Material	E_X^b (meV)	E_{loc} (meV)	w (meV)	Reference
p-GaAs	5	3		[48]
ZnTe : P	13	11		[38]
n-GaN	27	6–7		[30, 35]
ZnO : Al	59	15		[37]
$Al_{0.24}Ga_{0.76}As$: C	5.4	3.5	5.2	[5]
$Al_{0.23}Ga_{0.77}N$: Si	~ 40	10	30	[24]
$Mg_{0.11}Zn_{0.89}Te$: P			11	[40]
$Mg_{0.06}Zn_{0.94}O$: Al	55	28	20	This work

due to (cation) disorder, e.g. for (Al,In)As [22], (Al,Ga)N [14], [23–25] (Mg,Zn,Cd)Se [26] or (Mg,Zn)O [13, 27, 28]. We note that, generally, exciton localization, of course, plays a role only for temperatures at which excitons are stable. For GaAs the exciton binding energy E_X^b of about 4 meV [29] limits excitonic effects to low temperatures. Wide-gap semiconductors like GaN (ZnO) with E_X^b of 27 meV [30] (59 meV [31]) exhibit excitonic recombination at or above room temperature.

Another well-known localization mechanism of excitons in semiconductors is the binding to neutral shallow point defects (impurities or structural defects), observable as additional spectral lines [32]. These lines, (D^0,X) and (A^0,X), for excitons bound to neutral donors and acceptors (BX), respectively, are quite sharp ($\ll 1$ meV) at liquid helium temperature in binary semiconductors such as GaAs, GaN or ZnO. The recombination peak energy is given by $E_{BX} = E_X - E_{loc}$. The energy E_{loc} to remove an exciton from a neutral impurity is related to the impurity ionization energy, the binding energy E_D^b (E_A^b) for an electron (hole) on the donor (the acceptor). Hayne's rule $E_{loc}/E^b \approx 0.1$ has been established for donors and acceptors in silicon [33]. Modified rules have been reported for other semiconductors. An overview of the exciton binding energy, impurity localization energy and full-width at half-maximum ($w = 2.36\,\sigma$, best known values) of low-temperature recombination for various binary compound semiconductors and ternary alloys is given in table 1. Typical values for E_{loc} are about 1 meV for donors in GaAs [34], 6–7 meV for donors in GaN [35, 36] and 15 meV [37] for ZnO : Al. In alloys with small broadening effects BX emission is routinely observed, e.g. for (Zn,Cd)S, (Zn,Cd)Se and (Zn,Cd)Te within the entire composition range [7] and for $Mg_xZn_{1-x}Te$ up to at least $x = 0.2$ [39, 40]. In alloys with large inhomogeneous broadening (and at finite temperatures, additionally homogeneous broadening) such as (Al,Ga)N and (Mg,Zn)O, the BX and FX recombination peaks cannot be spectrally separated and the recombination is attributed in the literature to disorder localized excitons only as mentioned above. Only in [41] the low-temperature recombination in $Al_{0.5}Ga_{0.5}N$: Si has been attributed to donor-bound excitons.

In this paper, we demonstrate that exciton localization in semiconductor alloys is generally due to competing mechanisms of localization due to disorder and localization on shallow point defects. Both effects must be considered to interpret and evaluate the temperature dependence of exciton localization. Since shallow defects are ubiquitous also in other alloys, our results are of general importance.

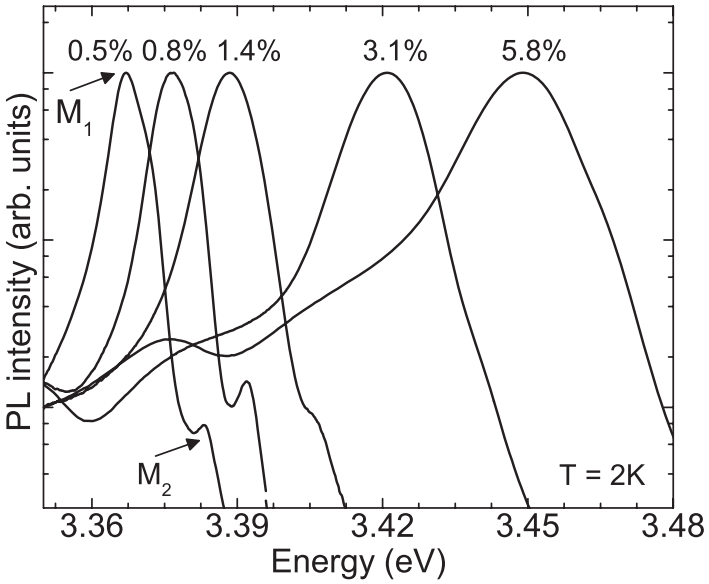

Figure 1. PL spectra (scaled to the same maximum) at $T = 2$ K of $Mg_xZn_{1-x}O$ thin films with different Mg contents x as labeled. The maxima M_1 and M_2 are indicated for the spectrum of the sample with $x = 0.005$.

We use $Mg_xZn_{1-x}O$ ($x < 0.1$) as a model system. $Mg_xZn_{1-x}O$ provides the possibility to tune the band gap from 3.4 to 4.5 eV [42] by the incorporation of Mg atoms into the cation lattice sites [43]. The alloy has wurtzite structure up to Mg-content $x \approx 0.36$ [44]. $Mg_xZn_{1-x}O$ possesses an exciton binding energy far above the thermal energy at room temperature, at least 50 meV for $x = 0.17$ [12]. Therefore, excitonic recombination dominates the PL spectra beyond room temperature.

2. Experimental details

The investigated $Mg_xZn_{1-x}O$ thin films were grown by pulsed-laser deposition (PLD) in an oxygen atmosphere ($p(O_2) = 0.016$ mbar) at about 700 °C on $(11\bar{2}0)$-oriented sapphire with an $Mg_{0.4}Zn_{0.6}O$ buffer layer. The incorporation of Mg into the thin films was varied via the composition of the ablation target made from a mixture of ZnO and MgO powders. A ZnO control sample was grown from a pure ZnO target. PL measurements were performed in an He bath cryostat at 2 K and in a temperature-variable He flow cryostat for measurements between 5 and 290 K. The luminescence was excited with the 325 nm line of a continuous wave HeCd laser, spectrally decomposed by a 320 mm focal length monochromator with a 2400 lines mm^{-1} grating and detected with a Peltier-cooled GaAs photomultiplier. The minimal spectral bandwidth is 0.06 nm. The Mg-content of the thin films was determined performing energy dispersive x-ray analysis with an electron beam acceleration voltage of 3 kV, not penetrating the buffer layer.

3. Results and discussion

PL spectra at $T = 2$ K of $Mg_xZn_{1-x}O$ samples with Mg content ranging from $x = 0.005$ to 0.058 are depicted in figure 1(a). The PL maxima shift toward higher energies with increasing

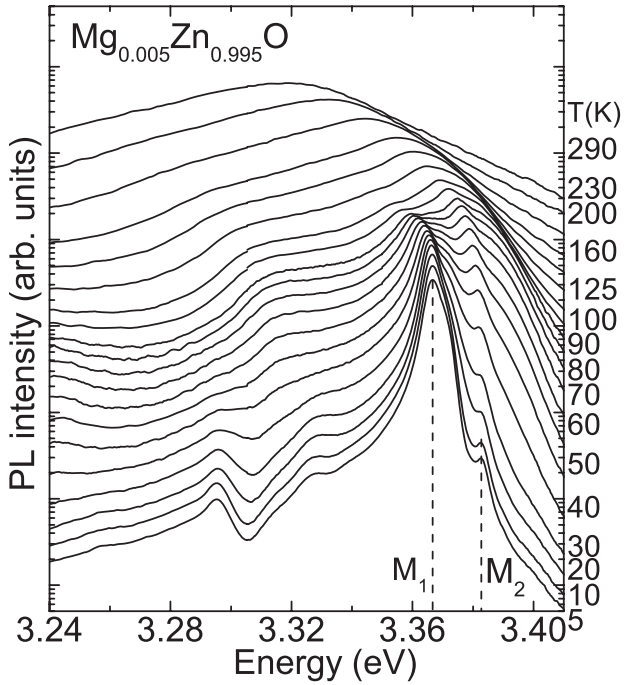

Figure 2. Temperature-dependent PL spectra between 5 and 290 K of an $Mg_{0.005}Zn_{0.995}O$ thin film. The spectra are shifted vertically for clarity. The position of the maxima M_1 and M_2 at low temperature is indicated by dashed lines.

Mg content due to a change of the alloy band gap. A linear fit of the experimental data for 18 samples[2] with $0 \leqslant x \leqslant 0.09$ yields $\partial E_{PL}/\partial x = 2.0\,eV$ at $T = 2\,K$. For $x = 0$ the dominant PL line has an energy of 3.3601 eV at $T = 2\,K$. This value is attributed to the transition of neutral Al-donor BX (the I_{6a} line) [45]. For $T = 300\,K$ the recombination peak is at 3.309 eV and resembles the energy for the transition of FX (the X_A line) in undoped ZnO [12].

The PL spectra of the (Mg,Zn)O thin films at 2 K show different peaks. The two dominating maxima are labeled M_1 and M_2 (figure 1(a)). The peak M_1 can be observed for all investigated samples at low temperatures. It is due to the recombination of excitons bound to neutral Al-donors (Al_{Zn}). FX (maximum M_2) dominate the PL spectra above 100 K up to room temperature. Such behavior is similar in pure ZnO. The peak separation of M_1 and M_2 is $E_{loc} = 15\,meV$ for $x = 0.005$, the same value as for (Al^0,X) in pure ZnO [37]. From Hall-effect studies on our PLD ZnO on Al_2O_3, we find a moderate Al concentration of typically several $10^{16}\,cm^{-3}$, stemming from the substrate [46]. We assume a similar concentration in our (Mg,Zn)O samples; however, Hall measurements cannot be performed due to larger compensation. We note that our PLD process on ZnO substrate yields only $[Al] = 3 \times 10^{13}\,cm^{-3}$ [47]. In figure 2 the temperature-dependent PL spectra of the $Mg_xZn_{1-x}O$ thin film with $x = 0.005$ are shown. The temperature was varied between 5 and 290 K. The maximum M_1 decreases in intensity with increasing temperature owing to the finite localization energy of BX. The activation energy for the intensity decrease [48] is found to be about $E_T = 16\,meV$, similar to E_{loc}. We note that the peak M_1 has obviously an asymmetric lineshape for a Mg content $x = 0.005$ with a shoulder at its

[2] For some of the samples, the Mg content has been varied via the oxygen partial pressure during growth.

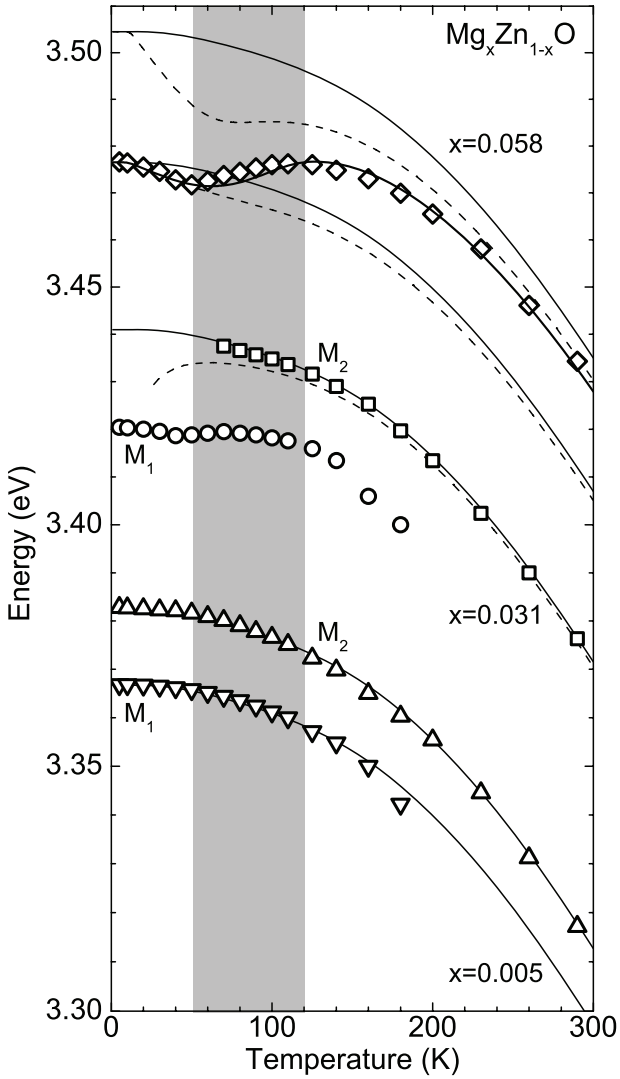

Figure 3. PL peak energy versus temperature for $Mg_xZn_{1-x}O$ thin films with $x = 0.005$, 0.031 and 0.058. The shaded area indicates the region for exciton delocalization. The solid lines indicate the temperature-dependent band-gap shift of ZnO. The dashed line for $x = 0.031$ indicates $S = S_0$. For $x = 0.058$, the dashed lines indicate the shift for free and bound excitons and the thick solid line, $E_{PL}(T)$, is from lineshape theory.

high-energy side. This is caused by another excitonic recombination process. The recombination of Zn_i donor bound excitons (the I_{3a} line) [49] is typical for PLD grown ZnO thin films [46].

We emphasize that due to sizable alloy broadening the recombination of BX and FX cannot be spectrally resolved in $Mg_xZn_{1-x}O$ for $x > 0.04$. This is also the typical situation for other semiconductor alloys when only one (broad) PL peak is observed for all temperatures.

For $Mg_xZn_{1-x}O$ thin films with $x = 0.005$ ($\sigma = 2.6$ meV) and 0.031 ($\sigma = 5.1$ meV), the energetic positions of the maxima M_1 and M_2 are resolved and depicted in figure 3. For $x = 0.005$, both peaks follow the temperature-dependent shift of the band gap of ZnO (solid lines) without significant localization effects. For $x = 0.031$, the spectral position of maximum M_1 (BX) undergoes a slight S-shape behavior with increasing temperature, indicating a small

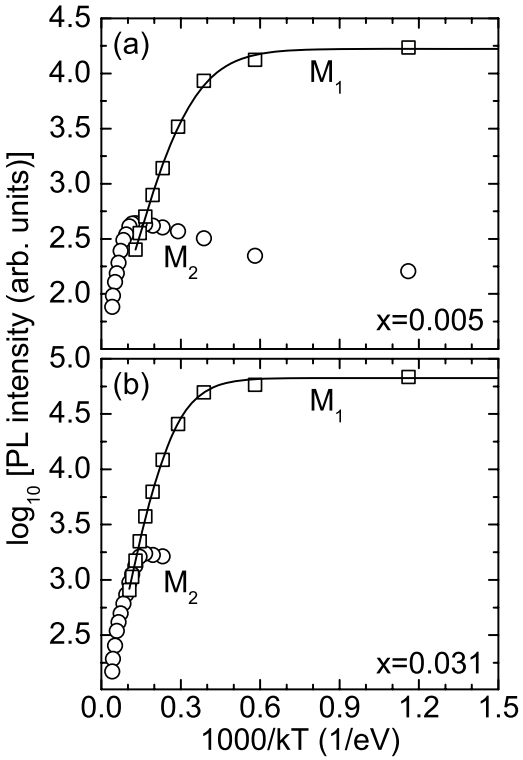

Figure 4. Integrated PL intensity of maxima M_1 and M_2 versus inverse temperature for $Mg_xZn_{1-x}O$ thin films with (a) $x = 0.005$ and (b) $x = 0.031$ as labeled. The solid lines depict fits for M_1 with equation (2). Fit parameters are given in table 1.

redistribution within the BX population. The FX recombination (M_2) follows the ZnO band-gap shift (solid line). The thermalization effect is much smaller than S_0 (dashed line). The extrapolated value for low temperatures indicates $E_{loc} = 21$ meV, in agreement with the thermal activation temperature of BX luminescence.

For $x = 0.058$, alloy broadening is so strong ($\sigma = 8.5$ meV) that the maxima M_1 and M_2 cannot be resolved individually. The spectral position of the PL maximum as a function of temperature is shown in figure 3. The PL maximum position undergoes a strong S-shape with increasing temperature. The peak character apparently changes from (D^0,X) to X_A with increasing temperature. Therefore we observe in this alloy at low temperature exciton localization on donors and *not* due to alloy disorder. A qualitatively similar shift is found for $x = 0.09$ in [28]. Attribution of the shift to alloy disorder only and evaluation with equation (1) [13, 24, 25, 27, 28] misses the true nature of the exciton localization mechanism.

Extrapolating E_X below 200 K with the ZnO band-gap shift yields $E_{loc} \approx 28$ meV for $x = 0.058$. Again, the decrease of intensity is found experimentally to have the same activation energy E_T. A lineshape model considering the ionization of BX can explain the $E_{PL}(T)$ dependence quite well (thick solid line); details will be published elsewhere. Our main conclusion is that the blue-shift in the temperature range 50–120 K is due to exciton ionization from impurities and not due to 'unfreezing' of excitons localized in the disorder potential.

As shown in figure 4, the temperature dependence of the PL intensity of the maxima M_1 and M_2 behaves similar for $x = 0.005$ and 0.031. The decrease in intensity with increasing

Table 2. Mg concentration x, fitted thermal activation energy E_T, localization energy E_{loc} and PL linewidth σ ($T = 2$ K) for various $Mg_xZn_{1-x}O$ samples.

x	E_T (meV)	E_{loc} (meV)	σ (meV)
0.000	16.3	–	–
0.005	16.5	15	2.6
0.008	17.9	16	3.0
0.014	18.8	18	3.8
0.031	22.0	21	5.1
0.058	27.0	(est.) 28	8.5

temperature of peak M_1 can be explained by the ionization of donor-bound excitons into neutral donors and FX. The temperature dependence of the integrated intensity of M_1 can be fitted using the formula [48] (solid line in figure 3)

$$I(T) = \frac{I_0}{A \exp(-E_T/k_B T) + 1}, \tag{2}$$

with I_0 being the intensity at $T = 0$ K, A being a dimensionless prefactor and E_T being the thermal activation energy of the participating (D^0,X) complexes. The fitted activation energies E_T as well as the determined localization energies E_{loc} are listed in table 2 for the $Mg_xZn_{1-x}O$ thin films of figure 1. At about 100 K both peaks have a similar weight, determining the transition temperature from dominating bound to dominating FX recombination. Table 2 shows an increase of E_{loc} and E_T with increasing Mg content, implying an increase of the binding energy of the donor involved. This phenomenon amplifies the observed S-shape for samples with Mg contents above $x = 0.058$, because the change of the dominant transition spans over a larger energy range for larger Mg contents.

We note that these mechanisms should be also present in doped ternary alloys. Dopants themselves can cause a shift of band gap with associated fluctuations and broadening, if present in sufficient concentration [50, 51]. However, in our nominally undoped samples, impurity concentrations are so small that such effects are not present.

4. Conclusion

From our analysis, we draw conclusions for two types of exciton localization in alloys: localization on shallow point defects at low temperatures (compared to E_{loc}/k_B) and localization in alloy disorder potential. The latter is observable at low temperatures for small broadening ($w < E_{loc}$), e.g. in (Zn,Cd)Se, and generally for $T > E_{loc}/k_B$. Both channels cannot be separately observed for large broadening $w > E_{loc}$ and a complex dependence $E_{PL}(T)$ develops. Three regimes exist: the 'S-shape' is due to FX localization in disorder potential for $E_{loc} \ll S$ (regime I) or due to impurity-bound exciton ionization for $E_{loc} \gg S$ (regime III). For $E_{loc} \sim S$ (intermediate regime II), as in this work, a more detailed analysis is necessary. We have compiled material parameters for a few alloys with large broadening in table 1, showing that e.g. (Al,Ga)As, (Al,Ga)N, (Mg,Zn)Te and (Mg,Zn)O belong to regime II.

Acknowledgments

We thank H Hochmuth for growing the investigated samples and G Ramm for target preparation. This work was supported by the Deutsche Forschungsgemeinschaft in the framework of Schwerpunktprogramm SPP1136 (Gr 1101/10-3), by the European Social Fund (ESF) and the Freistaat Sachsen.

References

[1] Adachi S 2009 *Properties of Semiconductor Alloys* (Chichester: Wiley)
[2] Goede O, John L and Hennig D 1978 *Phys. Status Solidi b* **89** K183
[3] Zimmermann R 1990 *J. Crystal Growth* **101** 346
[4] Zunger A and Mahajan S 1994 Atomic ordering and phase separation in III–V alloys *Handbook of Semiconductors* vol 3 (Amsterdam: Elsevier) p 1399–513
[5] Schubert E F, Göbel E O, Horikoshi Y, Ploog K and Queisser H J 1984 *Phys. Rev.* B **30** 813
[6] Langer J M, Buczko R and Stoneham A M 1992 *Semicond. Sci. Technol.* **7** 547
[7] Permogorov S and Reznitsky A 1992 *J. Lumin.* **52** 201
[8] Nakamura S, Mukai T and Senoh M 1994 *Appl. Phys. Lett.* **64** 1687
[9] Coli G and Bajaj K K 2001 *Appl. Phys. Lett.* **78** 2861
[10] Onuma T, Chichibu S F, Uchinuma Y, Sota T, Yamaguchi S, Kamiyama S, Amano H and Akasaki I 2003 *J. Appl. Phys.* **94** 2449
[11] Jiang L F, Shen W Z and Guo Q X 2009 *J. Appl. Phys.* **106** 013515
[12] Schmidt R *et al* 2003 *Appl. Phys. Lett.* **82** 2260
[13] Heitsch S *et al* 2007 *J. Appl. Phys.* **101** 083521
[14] Nepal N, Li J, Nakarmi M L, Lin J Y and Jiang H X 2006 *Appl. Phys. Lett.* **88** 062103
[15] Seppänen T, Hultman L and Birch J 2006 *Appl. Phys. Lett.* **89** 181928
[16] Suslina L G, Fedorov D L, Areshkin A G and Melekhin V G 1985 *Solid State Commun.* **55** 345
[17] Runge E 2002 *Excitons in Semiconductor Nanostructures in Solid State Physics* vol 57, ed H Ehrenreich and F Spaepen (San Diego, CA: Academic) pp 149–305
[18] Xu Z, Lu Z, Yuan Z, Yang X, Zheng B, Xu J, Ge W, Wang Y, Wang J and Chang L 1998 *Superlattices Microstruct.* **23** 381
[19] Yang F, Wilkinson M, Austin E J and O'Donnell K P 1993 *Phys. Rev. Lett.* **70** 323
[20] Grundmann M, Heinrichsdorff F, Ledentsov N N and Bimberg D 1999 *Adv. Solid State Phys.* **8** 203
[21] Li Q, Xu S J, Cheng W C, Xie M H, Tong S Y, Che C M and Yang H 2001 *Appl. Phys. Lett.* **79** 1810
[22] Ferguson I T, Cheng T S, Sotomayor Torres C M and Murray R 1994 *J. Vac. Sci. Technol.* B **12** 1319
[23] Steude G, Meyer B K, Göldner A, Hoffmann A, Bertram F, Christen J, Amano H and Akasaki I 1999 *Appl. Phys. Lett.* **74** 2456
[24] James G R, Leitch A W R, Omnes F, Wagener M C and Leroux M 2004 *J. Appl. Phys.* **96** 1047
[25] Lee K B, Parbrook P J, Wang T, Ranalli F, Martin T, Balmer R S and Wallis D J 2007 *J. Appl. Phys.* **101** 053513
[26] Maksimov O, Wang W H, Samarth N, Muñoz M and Tamargo M C 2004 *Phys. Status Solidi b* **241** 495
[27] Murotani H, Yamada Y, Taguchi T, Ishibashi A, Kawaguchi Y and Yokogawa T 2008 *J. Appl. Phys.* **104** 053514
[28] Wassner T A, Laumer B, Maier S, Laufer A, Meyer B K, Stutzmann M and Eickhoff M 2009 *J. Appl. Phys.* **105** 023505
[29] Ulbrich R G 1985 *Adv. Solid State Phys.* **25** 299
[30] Steube M, Reimann K, Frohlich D and Clarke S J 1997 *Appl. Phys. Lett.* **71** 948
[31] Thomas D G 1972 *J. Phys. Chem. Solids* **15** 86
[32] Bebb H B and Williams E W 1972 *Semicond. Semimet.* **8** 321

[33] Haynes J R 1960 *Phys. Rev. Lett.* **4** 361
[34] Driessen F A J M, Lochs H G M, Olsthoorn S M and Giling L J 1991 *J. Appl. Phys.* **69** 906
[35] Viswanath A K, Lee J I, Kim D, Lee C R and Leem J Y 1998 *Appl. Phys.* A **67** 551
[36] Kornitzer K, Grehl M, Thonke K, Sauer R, Kirchner C, Schwegler V, Kamp M, Leszczynski M, Grzegory I and Porowski S 1999 *Physica* B **273-274** 66
[37] Meyer B K *et al* 2004 *Phys. Status Solidi b* **241** 231
[38] Wolf K, Worz M, Wagner H P, Kuhn W, Naumov A and Gebhardt W 1993 *J. Cryst. Growth* **126** 643
[39] El Akkad F, Demian S and Chevallier J 1985 *J. Mat. Sci.* **20** 165
[40] Saito K, Kinoshita K, Tanaka T, Nishio M, Guo Q and Ogawa H 2006 *Phys. Status Solidi c* **3** 812
[41] Wagener M C, James G R, Leitch A W R and Omnés F 2004 *Phys. Status Solidi c* **1** 2322
[42] Lorenz M *et al* 2003 *Solid State Electron.* **47** 2205
[43] Sharma A K, Narayan J, Muth J F, Teng C W, Jin C, Kvit A, Kolbas R M and Holland O W 1999 *Appl. Phys. Lett.* **75** 3327
[44] Ohtomo A, Kawasaki M, Koida T, Masubuchi K, Koinuma H, Sakurai Y, Yoshida Y, Yasuda T and Segawa Y 1998 *Appl. Phys. Lett.* **72** 2466
[45] Meyer B K, Sann J, Lautenschläger S, Wagner M R and Hoffmann A 2007 *Phys. Rev.* B **76** 184120
[46] von Wenckstern H, Weinhold S, Biehne G, Pickenhain R, Schmidt H, Hochmuth H and Grundmann M 2005 *Adv. Solid State Phys.* **45** 263
[47] von Wenckstern H *et al* 2007 *Phys. Status Solidi (RRL)* **1** 129
[48] Bimberg D, Sondergelb M and Grobe E 1971 *Phys. Rev.* B **4** 3451
[49] Sann J, Stehr J, Hofstaetter A, Hofmann D M, Neumann A, Lerch M, Haboeck U, Hoffmann A and Thomsen C 2007 *Phys. Rev.* B **76** 195203
[50] Ebert P, Zhang T, Kluge F, Simon M, Zhang Z and Urban K 1999 *Phys. Rev. Lett.* **83** 757
[51] Pearson G L and Bardeen J 1949 *Phys. Rev.* **75** 865